Boosting mesenchymal stem cells regenerative activities on biopolymers-calcium phosphate functionalized collagen membrane

Marie Dubus, Hassan Rammal, Halima Alem, Nicolae Bercu, Isabelle Royaud, Fabienne Quilès, Fouzia Boulmedais, Sophie C. Gangloff, Cédric Mauprivez, Halima Kerdjoudj

Article type: Full Paper

Boosting mesenchymal stem cells regenerative activities on biopolymers-calcium phosphate functionalized collagen membrane

Marie Dubus[1,2#], Hassan Rammal[1,2#], Halima Alem[3], Nicolae B. Bercu[4], Isabelle Royaud[3], Fabienne Quilès[5,6], Fouzia Boulmedais[7], Sophie C. Gangloff[1,8], Cedric Mauprivez[1,2,9], Halima Kerdjoudj[1,2*]

1. EA 4691, Biomatériaux et Inflammation en Site Osseux (BIOS), SFR CAP Santé (FED 4231), Université de Reims Champagne Ardenne, 51100 Reims, France.

2. UFR d'Odontologie, Université de Reims Champagne Ardenne, 51100 Reims, France.

3. Université de Lorraine, UMR 7198 CNRS, Institut Jean Lamour, 54011 Nancy, France.

4. EA 4682, Laboratoire de Recherche en Nanoscience (LRN), Université de Reims Champagne-Ardenne, 51100 Reims, France.

5. CNRS, Laboratoire de Chimie Physique et Microbiologie pour les Matériaux et l'Environnement, LCPME, UMR 7564, Villers-lès-Nancy F-54600, France.

6. Université de Lorraine, Laboratoire de Chimie Physique et Microbiologie pour les Matériaux et l'Environnement, LCPME, UMR 7564, Villers-lès-Nancy F-54600, France.

7. Université de Strasbourg, CNRS, Institut Charles Sadron, UPR22, 23 rue du Loess, BP 84047, 67034, Strasbourg Cedex 2, France.

8. UFR de Pharmacie, Université de Reims Champagne Ardenne, 51100 Reims, France.

9. Pôle Médecine bucco-dentaire, Hôpital Maison Blanche, Centre Hospitalier Universitaire de Reims, France.

[#] M. D. and H. R. contributed equally to this work

***Corresponding author:**

Dr. Halima KERDJOUDJ. EA 4691 « Biomatériaux et Inflammation en Site Osseux », Pôle Santé, UFR d'Odontologie, SFR-CAP Santé (FED 4231), URCA, 1 Avenue du Maréchal Juin, 51100 Reims, France.

E-mail: halima.kerdjoudj@univ-reims.fr.

Abstract:

The regeneration of bone-soft tissue interface, using functional membranes, remains challenging and can be promoted by improving mesenchymal stem cells (MSCs) paracrine function. Herein, a collagen membrane, used as guided bone regeneration membrane, was functionalized by calcium phosphate, chitosan and hyaluronic acid hybrid coating by simultaneous spray of interacting species process. Composed of brushite, octacalcium phosphate and hydroxyapatite, the hybrid coating increased the membrane stiffness by 50%. After 7 days of MSCs culture on the hybrid coated polymeric membrane, biological studies were marked by a lack of osteoblastic commitment. However, MSCs showed an enhanced proliferation along with the secretion of cytokines and growth factors that could block bone resorption and favour endothelial cell recruitment without exacerbating polynuclear neutrophils infiltration. These data shed light on the great potential of inorganic/organic coated collagen membranes as an alternative bioactive factor-*like* platform to improve MSCs regenerative capacity, in particular to support bone tissue vascularization and to modulate inflammatory infiltrates.

Keywords: Bone regeneration; Inorganic/organic hybrid coating; Human stem cells; Cytokines; Growth factors.

1. Introduction

Despite its intrinsic regeneration and self-repair capacity, bone large segmental defects, usually caused by severe trauma, tumor resection, infections or disorders associated pathologies, require surgical remediation using bone biomaterials. Guided Bone Regeneration (GBR), considered as one of the most attractive techniques to regenerate alveolar bone, consists in the application of an occlusive membrane that provides space maintenance, promoting bone regeneration and preventing soft tissue infiltration. Despite accumulating evidences that GBR technique predictably leads to bone regeneration, multiple drawbacks are still reported such as a lack of an adequate tissue vascularization, a membrane collapse or an early exposure and bacteria colonization(1)(2). To improve GBR outcome, various membrane functionalization with specific drugs including antibiotics(3), anti-inflammatory(4), chemoattractive and osteogenic growth factors (*i.e.* bone morphogenic protein-7)(5) have been proposed. Nevertheless, high-cost concerns and adverse effects related to uncontrolled drug release tempered the initial excitement(6). Porous structures with the optimal size of pores in the scaffolds, support growth of cells in bone regenerative applications(7)(8). Owing to their bioactive and osteoconductive intrinsic features, inorganic porous materials such as calcium phosphate (CaP), calcium carbonate, bioactive glass were introduced in the main bulk of GBR membranes to favor osteoblast adhesion and proliferation(9)(10)(11)(12). However, limitations due to harsh fabrication conditions still exist despite recent advances in additive manufacturing such as electrospinning or laser and inkjet printing(13). The fabrication of a mechanically stable and microscopically homogeneous bone side functionalized membrane still seems challenging.

Materials mimicking the structure of natural bone are thought to be promising for application in bone tissue engineering(14). Macromolecules like chitosan (CHI) and hyaluronic acid (HA)

are largely investigated in this context. CHI forms polycation-polyanion complexes in the presence of HA and its amino groups make it especially convenient for biomineralization process(15). Enrichment of polysaccharidic scaffolds and/or hydrogels by mineral such as calcium phosphate (CaP) or calcium carbonates was applied as material to support osteoblast adhesion and proliferation(16)(17). Although they are bioactive and osteoconductive, calcium carbonates, in contrast to CaP bone substitutes, present a chemical composition far from bone apatite. We recently demonstrated that the biophysical features of CaP/CHI/HA coated glass induce mesenchymal stem cells (MSCs) commitment into an osteoblastic lineage through mechanobiological signalling(18). In the present work, we performed the same functionalization on clinically relevant materials, *i.e.* polymeric collagen based GBR membranes, and used them as substrate for MSCs culture. Exhaustive physicochemical and mechanical insights into hybrid inorganic/organic coating are provided before testing its intrinsic biological features, in comparison to inorganic-coated and bare membranes. In contrast to our previous study, the hybrid inorganic/organic coated polymeric collagen based membrane did not induce a cell commitment but improved MSCs proliferation along with the secretion of mediators required for bone formation/vascularization. Owing to its appropriate physicochemical properties, such materials can be considered as a bioactive factor-*like* platform to improve MSCs regenerative capacity.

2. Experimental

2.1. Materials: Calcium nitrate ($Ca(NO_3)_2$,$4H_2O$), diammonium hydrogen phosphate ($(NH_4)_2HPO_4$), sodium dihydrogen phosphate hydrate (NaH_2PO_4), Tris(hydroxymethyl) aminomethane (Tris), calcium chloride hydrate ($CaCl_2$, $2H_20$), sodium chloride and chitosan (75–85% deacetylated, low molecular weight) from Sigma and hyaluronic acid (200 kDa) from Lifecore Biomedical were used without further purification. Salt solutions were prepared in ultrapure water (Millipore®). In the case of hybrid (*i.e.* CaP/CHI/HA) coating build-up, $CaCl_2$, $2H_2O$ (0.32 M) and chitosan 0.3 mg/mL were dissolved in NaCl (0.15 M)/HCl (2 mM) buffer at pH 4 whereas NaH_2PO_4 (0.19 M) and hyaluronic acid 0.3 mg/mL were prepared in NaCl (0.15 M) buffer at pH 10. In the case of inorganic (*i.e.* CaP) coating build-up, a calcium solution of $Ca(NO_3)_2 \cdot 4H_2O$ (0.32 M) and a phosphate solution of $(NH_4)_2HPO_4$ (0.2 M) were prepared in Tris buffer (10 mM Tris, pH 4 and pH 10 respectively). Polymeric collagen based membranes (Bio-Gide®) were provided from Geistlich Pharma® and biocompatible glue (R41 wood vinylic) was provided from BOSTIK®.

2.2. Coating build-up: An automated spraying device was used to functionalize Bio-Gide® membranes with both hybrid and inorganic coatings. This device is constituted of four identical Airbrushes VL (Paasche®, USA) nozzles. Each nozzle is pressurized by in-house compressed air line under a pressure of 1 bar and connected to solenoid valves. The spraying of the different solutions, following a chosen deposition sequence, is obtained by a succession of closings and openings of the valves controlled by homemade software. Three nozzles allow spraying of the calcium (with/without chitosan), the phosphate (with/without hyaluronic acid) and of the rinsing solutions. The fourth nozzle, free of solution, is used for the drying step. The Bio-Gide® membrane is mounted vertically on a mobile holder, allowing the drainage of solution excess. The holder was rotated at 150 *rpm* to obtain a homogenous deposition of the coating. Both calcium (with/without chitosan) and phosphate (with/without hyaluronic acid)

corresponding solutions were sprayed simultaneously, on the membrane, for 2 sec followed by a rinsing step of 2 sec with ultrapure water and a drying step of 2 sec under compressed air. These steps were repeated 50 times and polymer concentrations were adjusted after calculation of flows during spraying in order to keep a charge ratio hyaluronic acid/chitosan constant and equal to 0.7 to optimize the complex formation. Biocompatible glue was used in order to stick the polymeric collagen based membranes on an appropriate surface for biological experiments.

2.3. Substrate characterization:

2.3.1. Scanning electron microscopy with a field emission gun (FEG-SEM). FEG-SEM investigations were performed with a FEG-SEM (JEOL JSM-7900F, France), on coated polymeric collagen based membranes sputtered with thin gold–palladium film (JEOL ion sputter JFC 1100). Samples were previously dehydrated in graded ethanol solutions from 50 to 100% and desiccated in hexamethyldisilazane (HMDS, Sigma) for 10 min, then air-dried at room temperature. Images were acquired from secondary electrons at primary beam energy at 5 kV.

2.3.2. Transmission Electron Microscopy (TEM). TEM investigations were performed with a JEOL ARM 200F – Cold FEG TEM/STEM (point resolution 0.19 nm in TEM mode and 0.078 nm in STEM mode) fitted with a GIF Quatum ER. High-Resolution TEM (HR-TEM) pictures were performed with a JEOL ARM 200F – Cold FEG (point resolution 0.19 nm) fitted with a GIF Quatum ER. Samples were previously dehydrated in graded ethanol solutions from 50 to 100% for 10 min and embedded in epoxy resin (48.2% epon 812, 34% anhydride nadic methyl, 16.4% anhydride [2-dodecenyl] succinic, and 1.5% 2,4,6-tris dimethy- laminoethyl] phenol) for 72 h at 60°C. Ultra-thin cross sections (60 nm in thickness) were performed using an automatic ultra-microtome (Ultracut-UCT Ultramicrotome, Leica) at room temperature.

155 *2.3.3. X-ray photoelectron spectroscopy (XPS).* XPS spectra were obtained from XPS
156 ESCALAB 250 spectrometer (Thermo Scientific) equipped with a
157 monochromatized micro focused Monochromatic Al K source X-ray
158 source (powered at 15 kV). The pass energy was set at 20 eV. The sample is
159 placed on the standard sample holder and at an angle parallel to the
160 input lens axis. The flood gun was used for charge compensation (1 µA, 14 eV, Ar gas).
161 The C–(C, H) component of the C 1s peak of carbon has been fixed to 285 eV
162 to set the binding energy scale. Data treatment was performed with the
163 Advantage Software program. Some spectra were decomposed with the least
164 squares fitting routine provided by the software with a
165 Gaussian/Lorentzian (85/15, 70/30) product function and after subtraction
166 of a non-linear baseline. Atomic ratios were calculated using peak
167 areas normalized on the basis of acquisition parameters and sensitivity
168 factors provided by the manufacturer. For each condition, two coated polymeric
169 membranes were analysed on two different points.
170 *2.3.4. Infrared (IR) microspectroscopy.* IR spectra, in reflectance mode, were recorded
171 between 4000 and 800 cm^{-1} on a Bruker Vertex 70v spectrometer equipped with a Hyperion
172 2000 microscope and a (×15) objective controlled by OPUS 7.5 software. A KBr beam
173 splitter and a MCT detector were used. The resolution of the single beam spectra was 4 cm^{-1}.
174 Masks of 300 µm × 220 µm were used to record 18 spectra and obtain maps on a (1380 × 915
175 µm) of membrane analysed surface. The number of bidirectional double-sided interferogram
176 scans was 64, which corresponds to a 40 sec accumulation. All interferograms were Fourier
177 processed using the Mertz phase correction mode and a Blackman-Harris three-term
178 apodization function. Measurements were performed at 21 ± 1°C in an air-conditioned room.
179 Water vapor subtraction was performed when necessary, and baseline was corrected at 3800,
180 2500, 1900 and 900 cm^{-1} before further analysis of the spectra.

2.3.5. Dynamic Mechanical Analysis (DMA). Dynamic mechanical properties of functionalized polymeric collagen membranes were determined using a Netzsch DMA 242C. Measurements of the complex modulus were performed in tension mode at three different frequencies (1.5 and 10 Hz) in the temperature range of around 37 ± 1°C. The complex modulus is composed of the storage modulus E' (real part) and the loss modulus E'' (imaginary part). E' represents the stiffness of a viscoelastic material and is proportional to the energy stored during a loading cycle (20 µm amplitude). It is roughly equal to the elastic Young modulus. E'' represents the energy loss from the viscous part of the polymer. The loss factor $tan\,\delta$ is then defined as the ratio of the loss modulus to storage modulus.

2.4. Biocompatibility studies:

2.4.1. Wharton's jelly mesenchymal stem cells (MSCs). Human umbilical cord harvesting was approved ethically and methodologically by our local Research Institution and was conducted with informed patients (written consent) in accordance with the usual ethical legal regulations (Article R 1243-57). All procedures were done in accordance with our authorization and registration number DC-2014-2262 given by the National ''Cellule de Bioéthique''. MSCs were enzymatically isolated from fresh human umbilical cords obtained after full-term births. MSCs were amplified at density of 3×10^3 cell/cm^2 in α-MEM supplemented with 10% decomplemented FBS, 1% Penicillin/Streptomycin/Amphotericin B and 1% Glutamax® (*v/v*, Gibco) and maintained in a humidified atmosphere of 5% CO_2 at 37°C with a medium change every two days. MSCs were seeded in 24 well plates at 24,000 cells/cm^2 on UV-decontaminated (20 min) hybrid-coated membranes glued on glass coverslips. UV-decontaminated inorganic-coated and bare polymeric membranes glued on glass coverslips were used as control.

2.4.2. Mitochondrial activity. After 2, 4 and 7 days of culture on hybrid-coated polymeric membranes and on controls, WST-1 cell proliferation assay (Roche Diagnostics) was

performed on MSCs in accordance with the manufacturer protocol. Absorbance was measured at 440 nm using a FLUOstar Omega microplate reader (BMG Labtech) against a background control as blank. A wavelength of 750 nm was used as the correction wavelength.

2.4.3. DNA quantification. After 7 days of culture on hybrid-coated polymeric membranes and on controls, DNA was extracted using MasterPure™ DNA Purification Kit (Epicentre® Biotechnologies) in accordance with the manufacturer protocol. Extracted DNA was assessed by measuring the absorbance at 260 and 280 nm (Nanodrop®, Thermo Scientific) with 260/280 nm absorbance ratio for all measured samples comprised between 1.8 and 2.

2.4.4. Cytoskeleton staining. After 7 days of culture on hybrid-coated polymeric membranes and on controls, MSCs were fixed with 4% (w/v) paraformaldehyde (Sigma-Aldrich) at 37 °C for 10 min and permeabilized with 0.5% (v/v) Triton ×100 for 5 min. Alexa® Fluor-488 conjugated-Phalloidin® (1/100 dilution in 0.1% Triton ×100) was used to stain F-actin for 45 min at room temperature. Nuclei were counter-stained with 4,6-diamidino-2-phenylindole (DAPI, 100 ng/mL, 1/10 000 dilution) for 5 min. Stained cells were mounted and imaged by confocal laser scanning microscopy (CLSM, Zeiss LSM 710 NLO, 20× objective, Numerical Aperture 1.4, Germany).

2.4.5. Cytokines and growth factors release by ELISA. After 7 days of MSCs culture on hybrid-coated polymeric membranes and on controls, supernatants were collected and stored at -20°C, and samples were subsequently assessed in duplicate for each specific cytokine/growth factor. Secreted levels of osteoprotegerin (OPG), receptor activator of nuclear factor kappa-B ligand (RANKL), vascular endothelial growth factor (VEGF), bone morphogenic protein-2 (BMP-2) and interleukin-6 (IL-6) were assessed using human Duoset® osteoprotegerin/TNFRSF11B, TRANCE/RANKL/TNFSF11, VEGF, BMP-2 and IL-6 (R&D systems) respectively, according to the manufacturer's instructions. Secreted levels of interleukin-8 (IL-8) and basic fibroblast growth factor (b-FGF) were assessed by using human

ELISA MAX™ Deluxe Set IL-8 and FGF-basic (BioLegend®) respectively, according to the manufacturer's instructions. Optical densities were measured at 450 nm using a microplate reader (FLUOstar Omega microplate reader, BMG Labtech). Released amount of cytokines was calculated from the corresponding standard curves and normalized to total DNA content (measured using the DNA assay setup, Nanodrop, Thermo Scientific).

2.4.6. Neutrophils migration in Boyden chamber chemotaxis assay. Conditioned media from MSCs seeded on hybrid-coated polymeric membranes and on controls for 7 days were deposited on the lower compartment, whereas 5×10^4 neutrophils, collected as previously described(19), were seeded on a polycarbonate membrane (5 µm pores, Nucleopore Track-etch membrane, Whatman, Maidstone, UK) in the upper compartment. After 45 min of incubation at 37°C in 5% CO_2, non-migrating neutrophils were removed from the top of the membrane and migrated cells at the bottom were stained with May Grünwald Giemsa (RAL555 kit) and imaged (Axiovert 200M microscope, Zeiss, Oberkochen, Germany, Objective × 40). IL-8 solution (200 ng/mL) and MSCs culture medium were used as controls.

2.4.7. Endothelial cells migration through transwell cell migration assay. Conditioned media from MSCs seeded on hybrid-coated polymeric membranes and on controls for 7 days were deposited in a 24 well plastic culture plate, whereas 2×10^3 of human umbilical cord vein endothelial cells (HUVECs), isolated as previously described(20), were seeded on the top of a cell culture insert membrane (Millicell® Hanging Cell Culture Inserts). After 48h of incubation at 37°C in 5% CO_2, non-migrating HUVECs were removed from the top of the membrane and migrated cells at the bottom were fixed with methanol then stained with crystal violet. Migrated cells were imaged with an EVOS® digital microscope. HUVECs culture medium containing or not fetal bovine serum and MSCs culture medium were used as controls.

2.5. Statistical analysis: All statistical analysis were performed using GraphPad Prism 5

software. Biological experiments were performed with six independent umbilical cords in duplicate. Box plots represent median, 1st and 3rd quartiles, and 1st and 9th deciles, statistical analysis were performed using Mann & Whitney test. For each test, a value of $p < 0.05$ was accepted as statistically significant p (rejection level of the null-hypothesis of equal means).

3. Results and discussion

In the context of bone-soft tissue interface regeneration, we herein aimed to functionalize polymeric collagen based membrane (Bio-Gide®), a dental medical device, with calcium phosphate, chitosan and hyaluronic acid coating. The integration of both organic and inorganic compounds is proposed to improve properties or implement functionalities of material(21). Bio-Gide® membrane was functionalized by an inorganic/organic coating, using a straightforward method, the simultaneous spray of interacting species. This technique allows the asymmetric functionalization of the membrane, *i.e.* only the bone-facing side. In order to investigate the advantage of supplementing calcium phosphate with chitosan and hyaluronic acid biopolymers, inorganic (calcium phosphate) coated and bare collagen polymeric membranes were used as controls. We used the term "hybrid coating" to designate the calcium phosphate, chitosan and hyaluronic acid coating; and the term "inorganic coating" for the calcium phosphate coating.

Representative top views of hybrid-coated polymeric collagen membranes, observed by FEG-SEM, showed the presence of mineral structures with both granular and rod shapes (Figure 1A). In contrast to inorganic coating, hybrid coating-derived rods were wrapped in biopolymers film (Figure $1A_2$ red arrow) and exhibited a smaller size (≈ 8.5 × 4 μm *versus* 18 × 7 μm). A deeper characterization of the crystal structure was performed by HR-TEM

combined with electron diffraction (ED). Both coatings displayed a nanostructured network of interconnecting elliptical-shaped particles (Figure 1B). However, difference in coatings particles shake-up was noticed; highlighting the presence of multiple clustered crystals embedded in an amorphous matrix in case of the hybrid coating (Figure $1B_1$). The growth of crystals within a confined environment provided by the amorphous organic film hampered the quantification of their size. Inorganic coating-derived crystals exhibited a diameter of about 10-20 nm (Figure $1B_3$). In addition to the difference in particles shake-up, HR-TEM revealed the presence of crystalline structures suggesting the presence of both octacalcium phosphate and hydroxyapatite in hybrid coating whereas inorganic coating derived crystals exhibited hydroxyapatite phase as evidenced by ED. Hybrid coating displayed $(\bar{1}\bar{7}1)$, (109), (301) and (113) corresponding to the respective inter-planar distance of 0.25 and 0.21 nm, whereas inorganic coating showed (131) with a characteristic spacing of 0.21 nm (Figure $1B_2$ and $1B_4$) (according to joint committee on powder diffraction standards (JCPSD®) n°26-1065 and American mineralogist structure (AMS) data n°15). Collagen gap junction and mineral deposition, usually observed during *in vitro* biomineralization, in the presence of collagen(22) were not observed in our case. This is probably due to the collagen membrane features. Although HR-TEM combined with electron diffraction is currently considered as the "gold standard" technique for the determination of crystal structure for any given mineral, recent report showed a great instability of both amorphous calcium phosphate and octacalcium phosphate under beam, making this investigation inaccurate(23).

A: FEG-SEM

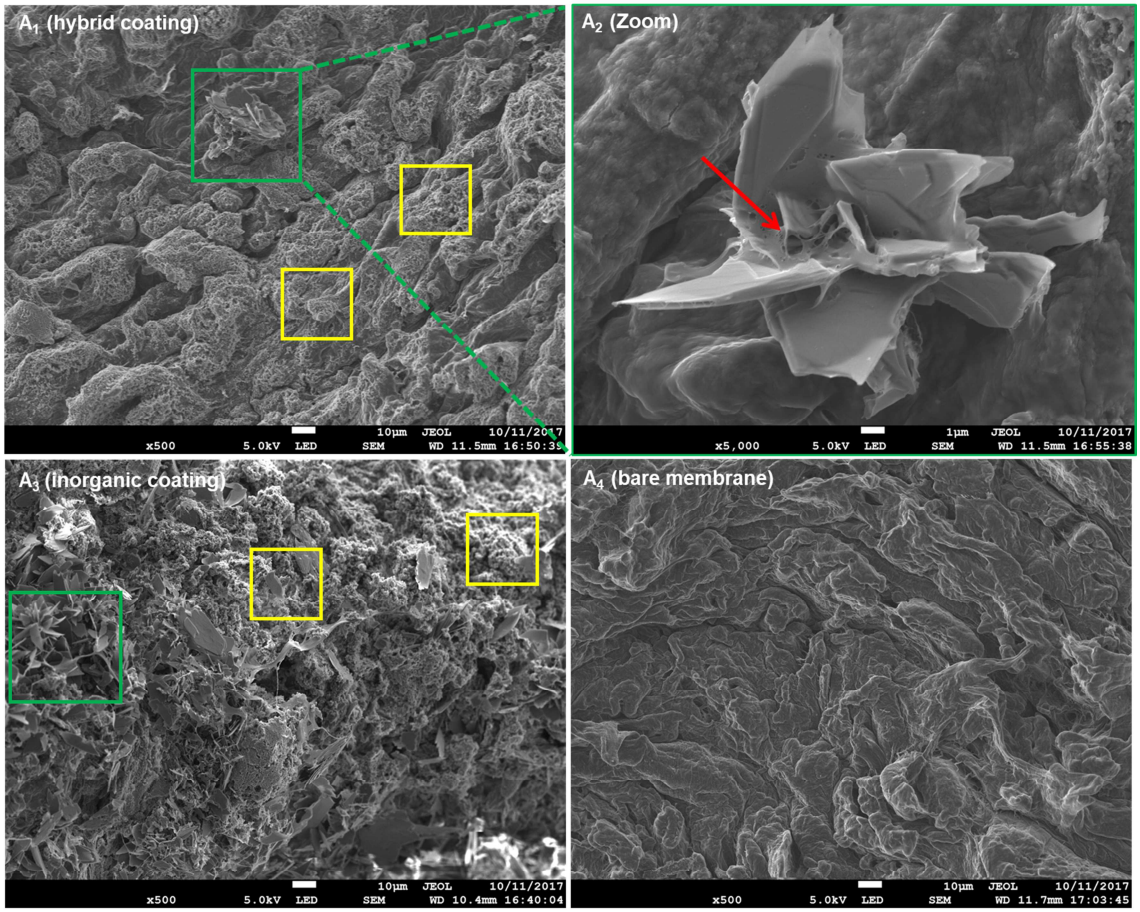

B: TEM/HR-TEM

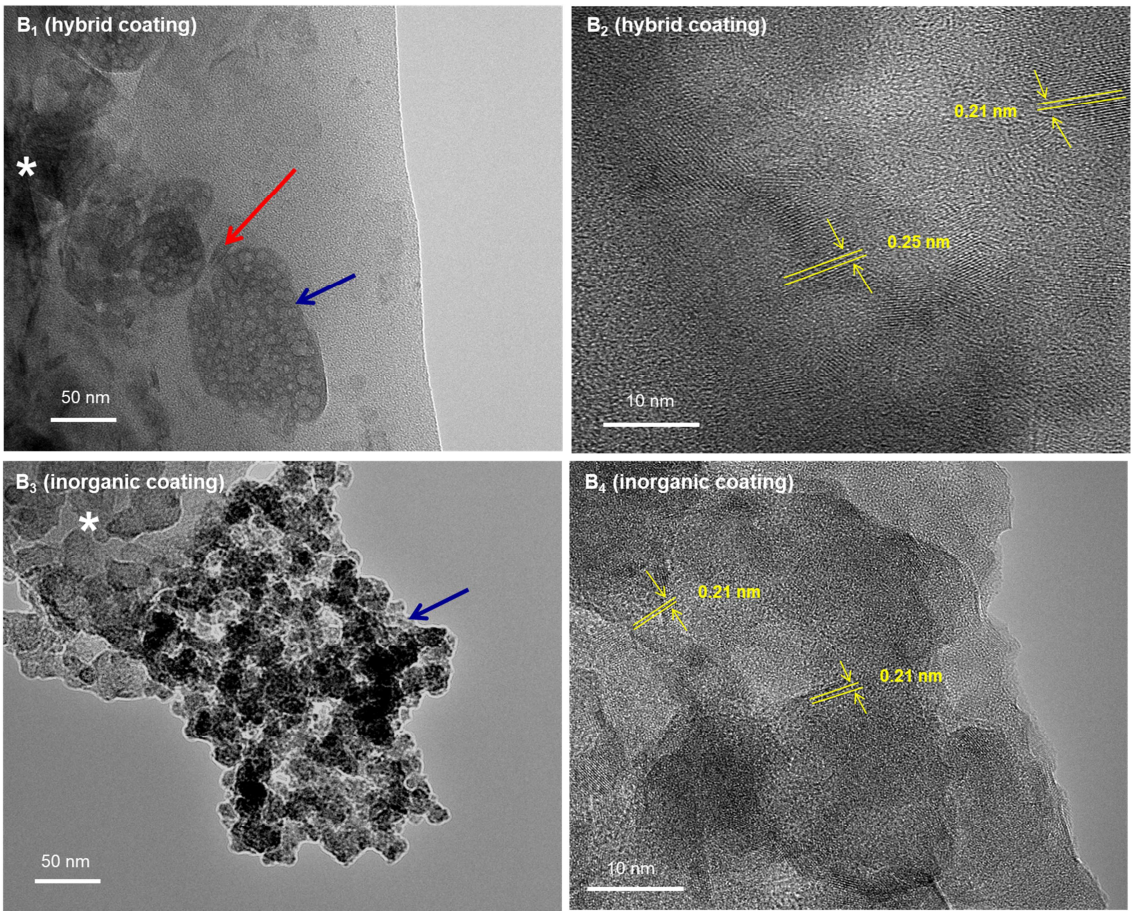

300

Figure 1: Surface morphology of hybrid and inorganic-coated membranes. A: Field Emission Gun-Scanning Electron Microscopy (FEG-SEM, scale bars = 10 and 1 μm) and B: Transmission Electron Microscopy (TEM) and High-Resolution (HR)-TEM (scale bars = 50 and 10 nm). Green and yellow squares show rod and granular shapes, respectively. Red and blue arrows indicate biopolymers film and minerals, respectively, whereas the stars highlight the polymeric collagen based membrane.

To gain more structural information, XPS and IR micro-spectroscopy were performed on both hybrid-coated and inorganic-coated polymeric membranes. Different biological calcium phosphate phases are known including hydroxyapatite, dicalcium phosphate dehydrate and octacalcium phosphate(24). XPS allows identifying the chemical composition on the extreme surface. Besides the prominent peaks corresponding to biopolymers (*i.e.* collagen, chitosan and hyaluronic acid) as C_{1s}, N_{1s} and also the O_{1s}, general XPS spectra showed calcium phosphate characteristic peaks, namely Ca_{2p}, P_{2p} and O_{1s} (Figure 2A). Although both coatings exhibited globally similar profiles, Ca/P atomic ratios were about 1.24 for the hybrid and 1.44 for the inorganic coating, which could be attributed to octacalcium phosphate and calcium-deficient hydroxyapatite, respectively. These values are consistent with the composition of the mineral phase observed during bone tissue formation, where the octacalcium phosphate phase is more abundant in the newly formed tissue and evolves toward a more crystalline carbonated hydroxyapatite phase, characteristics of mature bone matrix(25). Furthermore, *in vitro* biomineralization studies have demonstrated that the formation of hydroxyapatite as a final phase occurs through the conversion of an amorphous precursor phase into octacalcium phosphate *via* a cluster-growth mechanism(26). Many XPS studies reported that Ca/P atomic ratios of bone derived mineral (*i.e.* calcium-deficient hydroxyapatite) are lower than stoichiometric hydroxyapatite value (about 1.6), whereas O/Ca ratios are higher(27). In our case, the important contribution of biopolymers hindered the determination of a reliable O/Ca atomic ratio.

IR microspectrometry allows obtaining average spectra of both coatings. A slight variation in collagen bands intensities of the bare membrane was observed in comparison to known collagen peaks(28), probably due to the topography leading to weak variations of the focal point (Figure 2B). Collagen amide bands on both coated membranes appeared different in terms of shape and intensity (with a decrease of about 60%), comparing to bare collagen membrane; confirming the coating deposit. Data for main vibration bands from micro-infrared are compiled in Table 1 (Figure SI-1). Regarding chitosan and hyaluronic acid, their contributions are weak and overlap with hydroxyapatite, collagen and water peaks(9)(29). Thus, infrared analysis was focused on the area of spectra related to inorganic compounds (1200-950 cm^{-1}). This latter showed unexpected negative peaks, probably due to specific reflections of the IR beam on the uneven surface and to the poor crystalline state of mineral as previously described(30)(31). Inorganic-coated membranes exhibited bands assigned to mainly poorly crystalized carbonated hydroxyapatite. In contrast, hybrid-coated polymeric membrane showed several bands mainly assigned to dicalcium phosphate dehydrate(32). Raman spectra recorded on these samples were consistent with micro-infrared spectra, showing the same phosphate compounds (data not shown). Unsuccessful detection of poorly crystalized hydroxyapatite phase on the hybrid-coated polymeric membrane could be due to the uneven surface and/or to the shake-up of clustered crystals embedded within an amorphous matrix as shown in TEM experiments. In addition, XPS experiments revealed higher Ca/C and P/C ratios of respectively 26% and 31% for the hybrid-coated polymeric membranes in comparison to inorganic-coated ones, probably due the weak presence of carbonates.

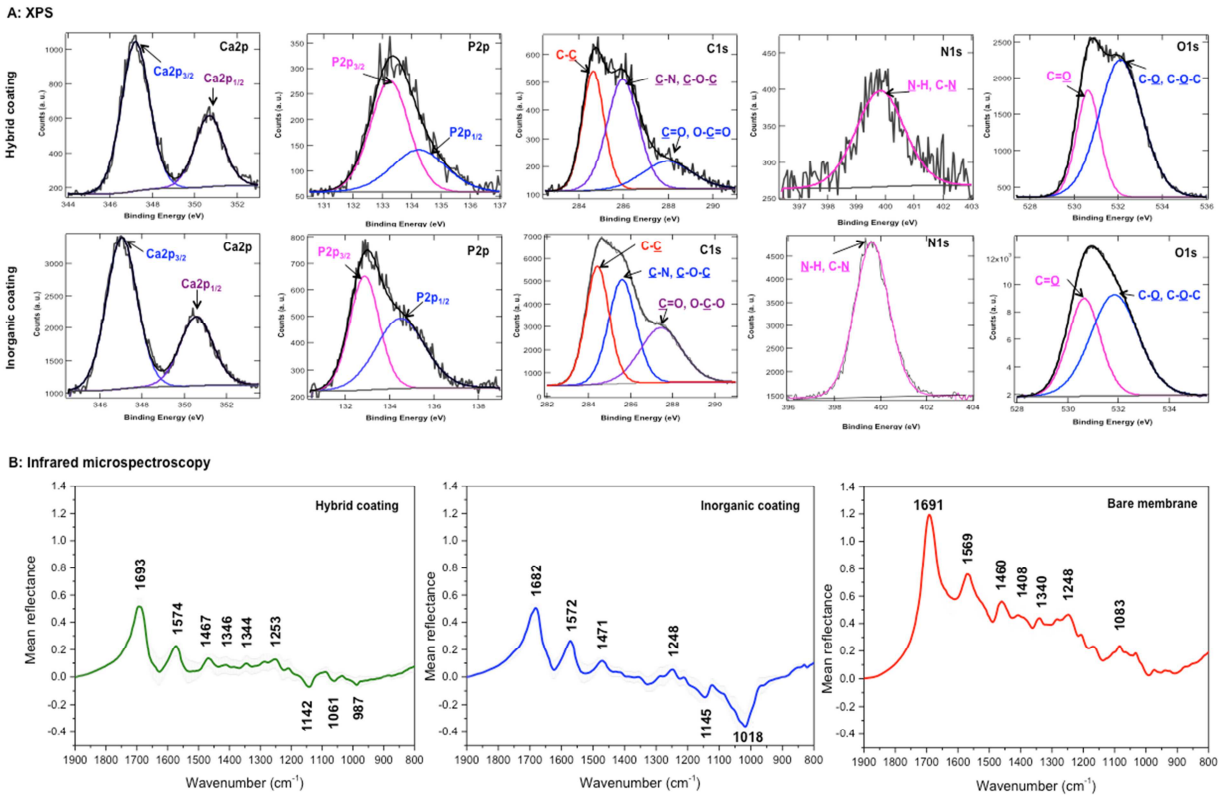

Figure 2: Chemical composition of hybrid and inorganic-coated membranes. A: X-rays photoelectron spectroscopy (XPS) of hybrid-coated polymeric collagen based membrane (upper line) and inorganic-coated polymeric collagen based membrane (lower line). B: Average spectra and standard deviation calculated from 18-recorded spectra obtained by Infrared micro-spectroscopy in reflectance mode, indicating the main peaks of dicalcium phosphate dehydrate for the hybrid-coated polymeric collagen based membrane and carbonated hydroxyapatite for the inorganic-coated polymeric collagen based membrane.

Table 1: Assignment of the main vibrational bands obtained by IR microspectroscopy (4000 - 800 cm^{-1}) on hybrid- and inorganic-coated polymeric collagen based membranes in comparison to bare membrane(28)

Infrared Wavenumber (cm^{-1})			Assignment	Associated compound
Hybrid coating	**Inorganic coating**	**Bare membrane**		
	~3630		νOH	Non-associated water
3538	3547		νOH	Weakly associated water
3488	3487	~3450	νOH	Water, COL
3369	3355	3347	νNH	COL
3091		3081	νCH, aromatics	
~2970		2964	νaCH_3	
		2934	νaCH_2	
2881		2877	νsCH_3	
~2130	~2125	~2130	OH and δOH combination	Water
1693	1682	1691	Amide I (νC=O)	COL
1643 (sh)	1641 (sh)	1640 (sh)	δH_2O	Water
1574	1572	1569	Amide II (νC-N, δNH)	COL
1467	1471	1460	δCH_n	
	1421		δCO3 (ν3)	Carbonate
1411		1408	νCOO^-	COL
1384		1389 (sh)	δCH_3	
	1355		δCO3 (ν3)	Carbonate
1344		1340	Amide III, ωCH_2, δCH_3	COL
1285	1286	1283	Amide III, ωCH_2, δCH_3	
1253	1248	1248	Amide III, ωCH_2, δCH_3	
1209	1212	1207	Amide III	
1142 (neg.)	1146 (neg.)			DCPD
		1083	νC-O	COL (carbohydrate moiety)
1061 (neg.)	1060 (neg.)			DCPD
	1036 (sh, neg.)	1032	νC-O	COL (carbohydrate moiety) HAp
	1017 (neg.)			HAp
987 (neg.)				DCPD

Key: ν: stretching, δ: bending, ω: wagging, a: antisymmetric, s: symmetric, sh: shoulder, DCPD: dicalcium phosphate dehydrate, COL: collagen, HAp: Hydroxyapatite.

Functionalized polymeric GBR membranes must possess adequate strength and elastic modulus to allow easy handling for their placement at the defect site and to avoid collapse under intraoral forces(33). Elastic modulus is the measure of a material stiffness, where a high elastic modulus reflects a stiff material while a low elastic modulus reflects a flexible one.

Blending of collagen with ceramics leads to enhancement of its mechanical properties(34). On the other hand, amalgamation with biopolymers confers toughness and flexibility to strong and hard calcium phosphate minerals(34). Thus, elastic moduli of hybrid- and inorganic-coated polymeric collagen based membranes were investigated by dynamic mechanical analysis (DMA) at 1 Hz under dry and wet conditions. Elastic moduli values of the membranes were higher in dry conditions, compared to wet conditions. Under wet condition, predicting the mechanical properties of the membrane *in vivo*, data in Table 2 indicate that the elastic moduli of hybrid- and inorganic-coated polymeric collagen based membrane, compared to bare membrane, were improved by more than 50% and 100% (Table 2). Moreover, a high flexibility and good handling of the hybrid-coated membrane were observed (Figure SI-2), which is useful for the tight attachment to curved surfaces in the context of GBR applications. Thus by incorporating calcium phosphate, chitosan and hyaluronic acid, we were able to functionalize dental polymeric collagen based collagen medical device and to improve its mechanical properties without affecting its flexibility and handling.

Table 2: Dynamic mechanical analysis under wet condition

	Hybrid coating	Inorganic coating	Bare membrane
E' (MPa)	1.8 ± 0.3	2.5 ± 0.2	1.2 ± 0.2

Recently, it was demonstrated that GBR membrane acts as a bioactive compartment, rather than merely a passive barrier. *In vivo*, GBR membrane attracts cells of different phenotypes, which sequentially express and secrete factors and signals favouring bone regeneration and remodelling (BMP-2, IL-6, b-FGF and TGF-β) and vascularization (VEGF)(35). Mesenchymal stem cells (MSCs) are a heterogeneous population, which exert their therapeutic effects by differentiating into osteoblasts and/or by secreting local soluble factors

required for bone regeneration. These soluble factors include interleukin (IL) -6 and -8, basic fibroblast growth factor (b-FGF), vascular endothelial growth factor (VEGF), bone morphogenic protein-2 (BMP)-2 and osteoprotegerin (OPG)(36)(37). Together, these secreted factors are known to dampen the inflammatory response, inhibit bone resorption and promote endothelial and osteoblast activities. Thus, it is necessary to check whether the membrane is able to support MSCs proliferation and function. Human MSCs were seeded and cytocompatibility of coated membranes was firstly assessed by WST-1 proliferation assay. Results showed that MSCs were metabolically active in contact with hybrid-coated membranes and both controls (inorganic-coated and bare membranes). An exponential increase in absorbance values from day 2 to 7 was observed for hybrid- and inorganic-coated polymeric collagen based membranes and a linear increase for bare membrane (Figure SI-3). In addition to WST-1 results showing an increase in metabolic activity of 23% (resp. 6%) for hybrid (resp. inorganic) coatings, DNA quantification at day 7 confirmed a higher MSCs content on both coated membranes (Figure 3A-B).

The differentiation of MSCs and the subsequent formation of bone are guided by several micro-environmental signals. We recently demonstrated that biophysical features of bone mimetic-coated glass (*i.e.* roughness and stiffness around 270 nm and 2 GPa, respectively), through mechanobiological signalling, carry away dramatic changes on MSCs morphology with polygonal cells exhibiting perpendicularly oriented F-actin fibres gathering around the nuclei, signature of osteoblastic commitment(18). In the present study, stained cytoskeleton showed a well elongated and flattened morphology where adhered MSCs displayed F-actin stress fibres parallel to the longitudinal cell axis whatever the studied condition (Figure 3C). Morphological studies highlighted MSCs fibroblastic shape, suggesting an uncommitted cell state.

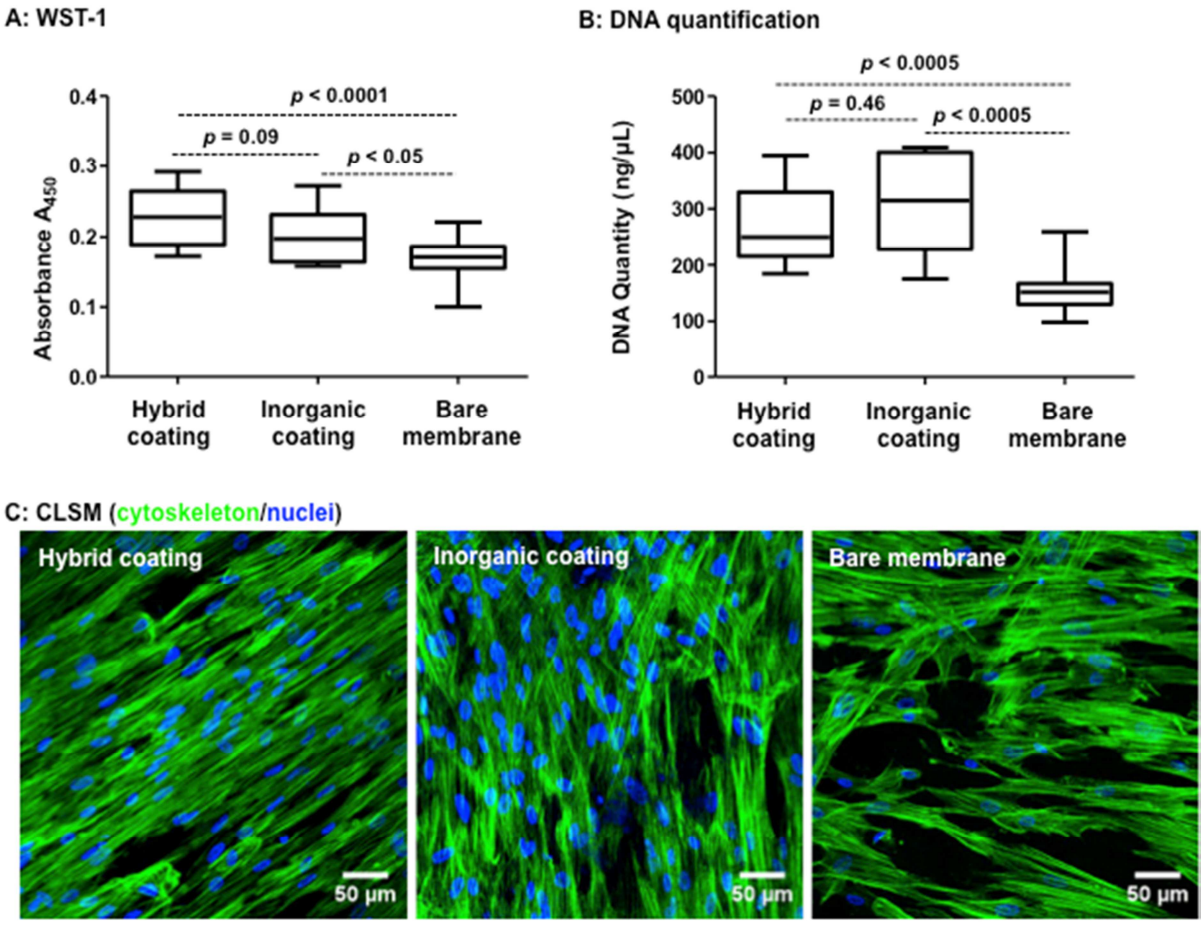

Figure 3: Biocompatibility of hybrid- and inorganic-coated polymeric collagen based membranes. A: WST-1 proliferation assay, B: DNA quantification and C: Confocal laser scanning microscopy (CLSM) fluorescent images of F-actin cytoskeleton (green colour) and nuclei (blue colour), confirming the higher cell proliferation on both coatings. (n=6, Mann & Whitney test, scale bars = 50 µm).

After a week of culture on coated and uncoated membranes, soluble factors secreted by MSCs were quantified by Enzyme-Linked Immunosorbent Assay (ELISA). BMP-2, described as a potent osteogenic factor secreted by bone cells, was not detected in supernatants in all tested conditions (Figure 4). However, we noticed a modest increase in IL-6 and IL-8 secretion by MSCs cultured on both coated membranes in comparison to bare membrane (Figure 4A and 4B). Pro-inflammatory cytokines TNF-α and IL-1β, known to harm bone regeneration, were below the detection limit whatever the investigated conditions. Although IL-6 and IL-8 are currently described as pro-inflammatory cytokines, a lack of exacerbated inflammatory

mediators release suggests that both hybrid- and inorganic-coated polymeric collagen based membranes offer a non-harmful environment for MSCs(19). Furthermore, IL-6 produced by MSCs is described to maintain their “stemness” and can also have an anti-inflammatory effect by limiting inflammatory infiltrates as neutrophils(38)(39). On the other hand, the basic biological role of IL-8 is attracting and activating neutrophils. Boyden-migration assays showed about 20% of neutrophils recruitment by MSCs conditioned media whatever the culture condition (Figure 4C), confirming then the neutral role of both coatings. Attractively, these inflammatory mediators are recently reported to be involved in natural regenerative process along with a great potential in bone repair treatment, through the regulation of osteoblasts and osteoclasts differentiation as well as angiogenesis(33)(40).

MSCs cultured on both hybrid- and inorganic-coated polymeric collagen based membranes released VEGF and b-FGF in a different manner compared to those cultured on bare membrane. VEGF release was moderately enhanced on hybrid- and significantly enhanced on inorganic-coating compared to bare membrane (Figure 4D). In contrast, b-FGF was significantly increased on both hybrid- and inorganic-coated polymeric collagen based membranes compared to bare membrane (Figure 4E). VEGF and b-FGF are known to contribute to vascularization(40). This latter was further confirmed through attraction of human umbilical vein endothelial cells (HUVECs) by MSCs conditioned media. Transwell chemotaxis assay showed that MSCs on hybrid- and inorganic-coated polymeric collagen based membranes enhanced HUVECs recruitment with about 85% and 97%, respectively (Figure 4F). MSCs on bare collagen membrane recruited only 3%. These results highlighted a superior angiogenic chemotaxis effect of MSCs cultured on hybrid- and inorganic-coated polymeric collagen based membranes.

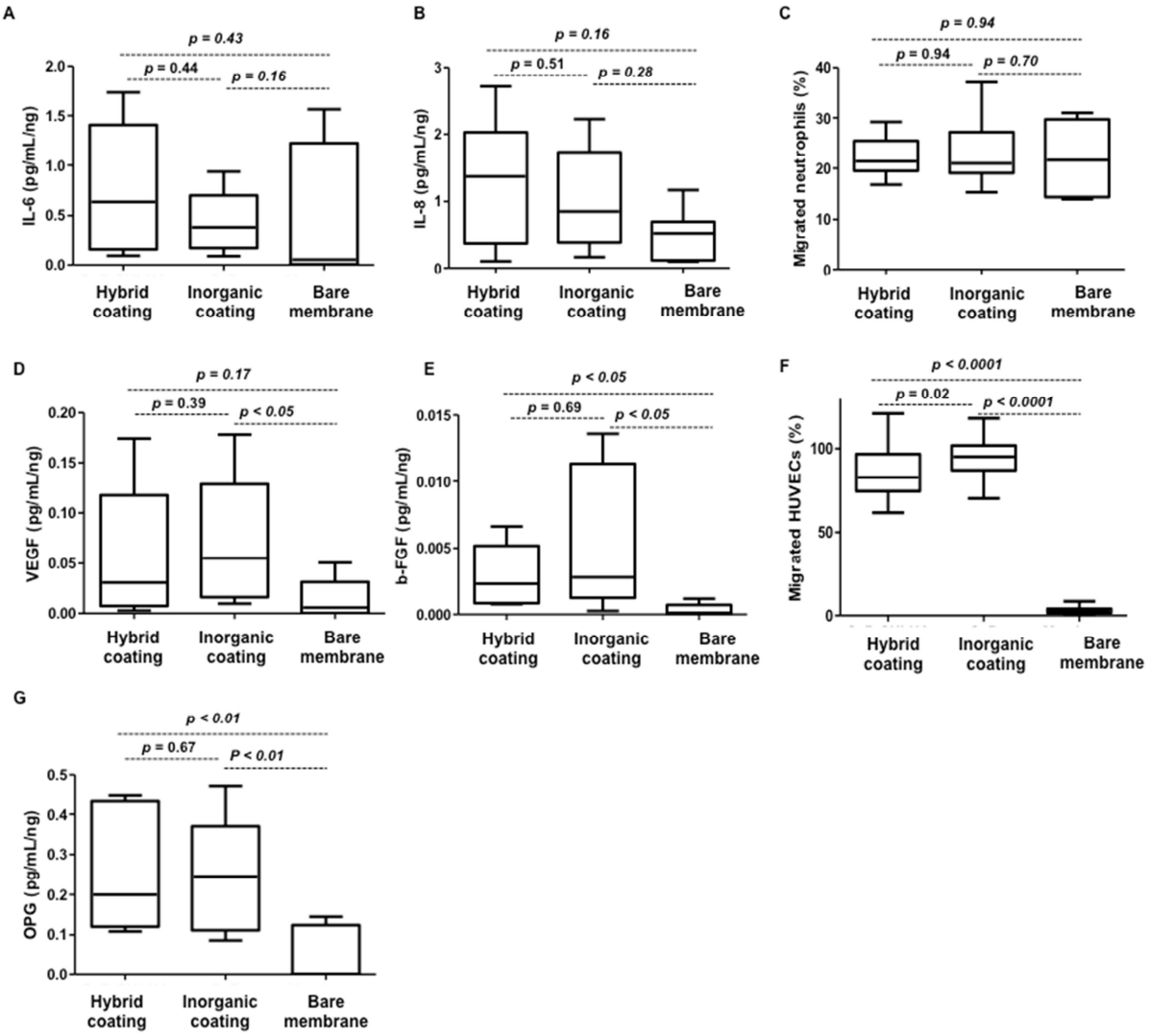

Figure 4: Paracrine activities of MSCs cultured on hybrid- and inorganic-coated polymeric collagen based membranes. A, B, D, E, G: ELISA quantification assay normalized to DNA content, C and F: Boyden and transwell migration assays of neutrophils and human umbilical vein endothelial cells (HUVECs) against MSCs conditioned media, respectively. Migrated neutrophils using IL-8 (200 ng/mL) and migrated HUVECs using endothelial growth medium were considered as 100%. (n=6, Mann & Whitney test).

The lack of BMP-2, as mentioned above, could be explained by the absence of osteoblast differentiation on both coated membranes. However, endothelial cells, in response to VEGF, are able to produce BMP-2, stimulating osteoblast recruitment/differentiation and promoting fracture healing(41)(42). Thus, despite a lack of MSCs commitment into osteoblastic lineage, our results suggest that hybrid- and inorganic-coated membranes could provide a local

environment favouring vascularization and subsequently bone formation. The receptor activator of nuclear factor kappa-B ligand (RANKL) is a soluble factor which induces osteoclasts (bone-resorbing cells) differentiation and activation through its binding to RANK. RANKL was not detected in supernatants whatever the studied conditions. Acting as a decoy receptor, OPG can prevent bone resorption by limiting RANKL/RANK interactions(43). OPG, constitutively produced by MSCs, was significantly increased on both hybrid and inorganic-coated membranes compared to bare membrane (Figure 4G). Taking together, these results suggest that both coatings could provide a local environment that blocks bone resorption.

3. Conclusion

We successfully functionalized the bone-facing side of polymeric collagen based membrane with brushite, octacalcium phosphate and hydroxyapatite combined with chitosan and hyaluronic acid biopolymers. The hybrid coating increased the membrane stiffness by 50% without affecting its flexibility and handling. The structural, chemical and mechanical features of the hybrid-coated polymeric collagen based membrane supported MSCs adhesion and function. Although no MSCs commitment into osteoblast lineage was observed after 7 days of culture, improvement in MSCs paracrine activities was achieved by promoting the secretion of inflammatory cytokines and pro-angiogenic growth factors, required for bone regeneration. The straightforward manufacturing process suggests that hybrid coating has a great potential for timely clinical translation in bone-soft tissue interface regeneration fields, including dentistry, craniofacial surgery, and orthopaedics.

Supporting Information: Supporting Information is available from ScienceDirect Online Library or from the author.

Conflicts of Interest: The authors declare no competing financial interest.

Acknowledgments: This work was partially supported by « Interreg V France-Wallonie-Vlaanderen program-TEXTOS ». Marie Dubus is supported by a doctoral fellowship from the High Education French Minister. Authors are very grateful to the staff of the Core PICT and NANOMAT (Dr. C. Terryn and Pr. M. Molinari) and Pr. P. Schaaf and Dr. J. Hemmerlé from INSERM U1121, Université de Strasbourg, France for SSCI setup and O. Godard and M. Ponçot from Institut Jean Lamour, Université de Lorraine, France for DMA technical assistance.

References:

1. Gruber R, Stadlinger B, Terheyden H. Cell-to-cell communication in guided bone regeneration: molecular and cellular mechanisms. Clin. Oral Implants Res. 28 (2017) 1139–1146.

2. Garcia J, Dodge A, Luepke P, Wang H-L, Kapila Y, Lin G-H. Effect of membrane exposure on guided bone regeneration: A systematic review and meta-analysis. Clin. Oral Implants Res. 29 (2018) 328–338.

3. Mathew A, Vaquette C, Hashimi S, Rathnayake I, Huygens F, Hutmacher DW, et al. Antimicrobial and Immunomodulatory Surface-Functionalized Electrospun Membranes for Bone Regeneration. Adv. Healthc. Mater. 6 (2017) 1601345.

4. Schwinté P, Mariotte A, Anand P, Keller L, Idoux-Gillet Y, Huck O, et al. Anti-inflammatory effect of active nanofibrous polymeric membrane bearing nanocontainers of atorvastatin complexes. Nanomed. 12 (2017) 2651–2674.

5. Schiavi J, Keller L, Morand D-N, Isla ND, Huck O, Lutz JC, et al. Active implant combining human stem cell microtissues and growth factors for bone-regenerative nanomedicine. Nanomed. 10 (2015) 753–763.

6. Jung RE, Thoma DS, Hammerle CHF. Assessment of the potential of growth factors for localized alveolar ridge augmentation: a systematic review. J. Clin. Periodontol. 35 (2008) 255–281.

7. Krok-Borkowicz M, Filova E, Chlupac J, Klepetar J, Bacakova L, Pamuła E. Influence of pore size and hydroxyapatite deposition in poly(l-lactide-co-glycolide) scaffolds on osteoblast-like cells cultured in static and dynamic conditions. Mater. Lett. 241 (2019) 1–5.

8. Murphy CM, Haugh MG, O'Brien FJ. The effect of mean pore size on cell attachment, proliferation and migration in collagen-glycosaminoglycan scaffolds for bone tissue engineering. Biomaterials. 31 (2010) 461–466.

9. Masoudi Rad M, Nouri Khorasani S, Ghasemi-Mobarakeh L, Prabhakaran MP, Foroughi MR, Kharaziha M, et al. Fabrication and characterization of two-layered nanofibrous membrane for guided bone and tissue regeneration application. Mater. Sci. Eng. C. 80 (2017) 75–87.

10. Chen Y-H, Tai H-Y, Fu E, Don T-M. Guided bone regeneration activity of different calcium phosphate/chitosan hybrid membranes. Int. J. Biol. Macromol. 126 (2019) 159–169.

11. Tokuda S, Obata A, Kasuga T. Preparation of poly(lactic acid)/siloxane/calcium carbonate

composite membranes with antibacterial activity. Acta Biomater. 5 (2009) 1163–1168.

12. Soltani Dehnavi S, Mehdikhani M, Rafienia M, Bonakdar S. Preparation and in vitro evaluation of polycaprolactone/PEG/bioactive glass nanopowders nanocomposite membranes for GTR/GBR applications. Mater. Sci. Eng. C. 90 (2018) 236–247.

13. Carter S-SD, Costa PF, Vaquette C, Ivanovski S, Hutmacher DW, Malda J. Additive Biomanufacturing: An Advanced Approach for Periodontal Tissue Regeneration. Ann. Biomed. Eng. 45 (2017) 12–22.

14. Li Y, Xiao Y, Liu C. The Horizon of Materiobiology: A Perspective on Material-Guided Cell Behaviors and Tissue Engineering. Chem. Rev. 117 (2017) 4376–4421.

15. Postnova I, Silant'ev V, Sarin S, Shchipunov Y. Chitosan Hydrogels and Bionanocomposites Formed through the Mineralization and Regulated Charging. Chem. Rec. 18 (2018) 1247–1260.

16. Douglas TEL, Łapa A, Samal SK, Declercq HA, Schaubroeck D, Mendes AC, et al. Enzymatic, urease-mediated mineralization of gellan gum hydrogel with calcium carbonate, magnesium-enriched calcium carbonate and magnesium carbonate for bone regeneration applications. J. Tissue Eng. Regen. Med. 11 (2017) 3556–3566.

17. Douglas TEL, Wlodarczyk M, Pamula E, Declercq HA, Mulder E de, Bucko MM, et al. Enzymatic mineralization of gellan gum hydrogel for bone tissue-engineering applications and its enhancement by polydopamine. J. Tissue Eng. Regen. Med. 8 (2014) 906–918.

18. Rammal H, Dubus M, Aubert L, Reffuveille F, Laurent-Maquin D, Terryn C, et al. Bioinspired Nanofeatured Substrates: Suitable Environment for Bone Regeneration. ACS Appl. Mater. Interfaces. 9 (2017) 12791–12801.

19. Aubert L, Dubus M, Rammal H, Bour C, Mongaret C, Boulagnon-Rombi C, et al. Collagen-Based Medical Device as a Stem Cell Carrier for Regenerative Medicine. Int. J. Mol. Sci. 18 (2017) 2210.

20. Rammal H, Harmouch C, Maerten C, Gaucher C, Boulmedais F, Schaaf P, et al. Upregulation of endothelial gene markers in Wharton's jelly mesenchymal stem cells cultured on polyelectrolyte multilayers. J. Biomed. Mater. Res A. 105 (2017) 292–300.

21. Saveleva MS, Eftekhari K, Abalymov A, Douglas TEL, Volodkin D, Parakhonskiy BV, et al. Hierarchy of Hybrid Materials—The Place of Inorganics-in-Organics in it, Their Composition and Applications. Front. Chem. 7 (2019) 179.

22. Beniash E. Biominerals- hierarchical nanocomposites: the example of bone. Wiley Interdiscip. Rev. Nanomed. Nanobiotechnol. 3 (2011) 47–69.

23. Drouet C. Apatite Formation: Why It May Not Work as Planned, and How to Conclusively Identify Apatite Compounds. BioMed. Res. Int. 2013 (2013) 490946.

24. Habraken W, Habibovic P, Epple M, Bohner M. Calcium phosphates in biomedical applications: materials for the future? Mater. Today. 19 (2016) 69–87.

25. Mechiche Alami S, Gangloff SC, Laurent-Maquin D, Wang Y, Kerdjoudj H. Concise Review: In Vitro Formation of Bone-Like Nodules Sheds Light on the Application of Stem Cells for Bone Regeneration. Stem Cells Transl Med. 5 (2016) 1587–1593.

26. Habraken WJEM, Tao J, Brylka LJ, Friedrich H, Bertinetti L, Schenk AS, et al. Ion-association complexes unite classical and non-classical theories for the biomimetic nucleation of calcium phosphate. Nat. Commun. 4 (2013) 1507.

27. Lu HB, Campbell CT, Graham DJ, Ratner BD. Surface Characterization of Hydroxyapatite and Related Calcium Phosphates by XPS and TOF-SIMS. Anal. Chem. 72 (2000) 2886–2894.

28. Belbachir K, Noreen R, Gouspillou G, Petibois C. Collagen types analysis and differentiation by FTIR spectroscopy. Anal. Bioanal. Chem. 395 (2009) 829–837.

29. Lei Y, Xu Z, Ke Q, Yin W, Chen Y, Zhang C, et al. Strontium hydroxyapatite/chitosan nanohybrid scaffolds with enhanced osteoinductivity for bone tissue engineering. Mater. Sci. Eng. C. 72 (2017) 134–142.

30. Vincent RK, Hunt GR. Infrared Reflectance from Mat Surfaces. Appl. Opt. 7 (1968) 53–59.

31. Hunt Graham R., Vincent Robert K. The behavior of spectral features in the infrared emission from particulate surfaces of various grain sizes. J. Geophys. Res. 73(2012) 6039–6046.

32. Koutsopoulos S. Synthesis and characterization of hydroxyapatite crystals: a review study on the analytical methods. J. Biomed. Mater. Res. 62 (2002) 600–612.

33. Chu C, Deng J, Sun X, Qu Y, Man Y. Collagen Membrane and Immune Response in Guided Bone Regeneration: Recent Progress and Perspectives. Tissue Eng. Part. B Rev. 23 (2017) 421–435.

34. Zhang D, Wu X, Chen J, Lin K. The development of collagen based composite scaffolds for bone regeneration. Bioact. Mater. 3 (2018) 129–138.

35. Turri A, Elgali I, Vazirisani F, Johansson A, Emanuelsson L, Dahlin C, et al. Guided bone regeneration is promoted by the molecular events in the membrane compartment. Biomaterials. 84 (2016) 167–183.

36. Popa G, Boulmedais F, Zhao P, Hemmerlé J, Vidal L, Mathieu E, et al. Nanoscale precipitation coating: the deposition of inorganic films through step-by-step spray-assembly. ACS Nano. 4 (2010) 4792–4798.

37. Haumer A, Bourgine PE, Occhetta P, Born G, Tasso R, Martin I. Delivery of cellular factors to regulate bone healing. Adv. Drug Deliv. Rev. 129 (2018) 285–294.

38. Pricola KL, Kuhn NZ, Haleem-Smith H, Song Y, Tuan RS. Interleukin-6 Maintains Bone Marrow-Derived Mesenchymal Stem Cell Stemness by an ERK1/2-Dependent Mechanism. J. Cell. Biochem. 108 (2009) 577–588.

39. Munir H, Luu N-T, Clarke LSC, Nash GB, McGettrick HM. Comparative Ability of Mesenchymal Stromal Cells from Different Tissues to Limit Neutrophil Recruitment to Inflamed Endothelium. PLoS ONE 11 (2016). 4865100.

40. Chim SM, Tickner J, Chow ST, Kuek V, Guo B, Zhang G, et al. Angiogenic factors in bone local environment. Cytokine Growth Factor Rev. 24 (2013) 297–310.

41. Zhang Y, Yang W, Devit A, Beucken JJJP van den. Efficiency of coculture with angiogenic cells or physiological BMP-2 administration on improving osteogenic differentiation and bone formation of MSCs. J. Biomed. Mater. Res. A 107 (2019) 643–653.

42. Kaigler D, Krebsbach PH, West ER, Horger K, Huang Y-C, Mooney DJ. Endothelial cell modulation of bone marrow stromal cell osteogenic potential. FASEB J. 19 (2005) 665–667.

43. Liu W, Zhang X. Receptor activator of nuclear factor-κB ligand (RANKL)/RANK/osteoprotegerin system in bone and other tissues. Mol. Med. Rep. 11 (2015) 3212–3218.

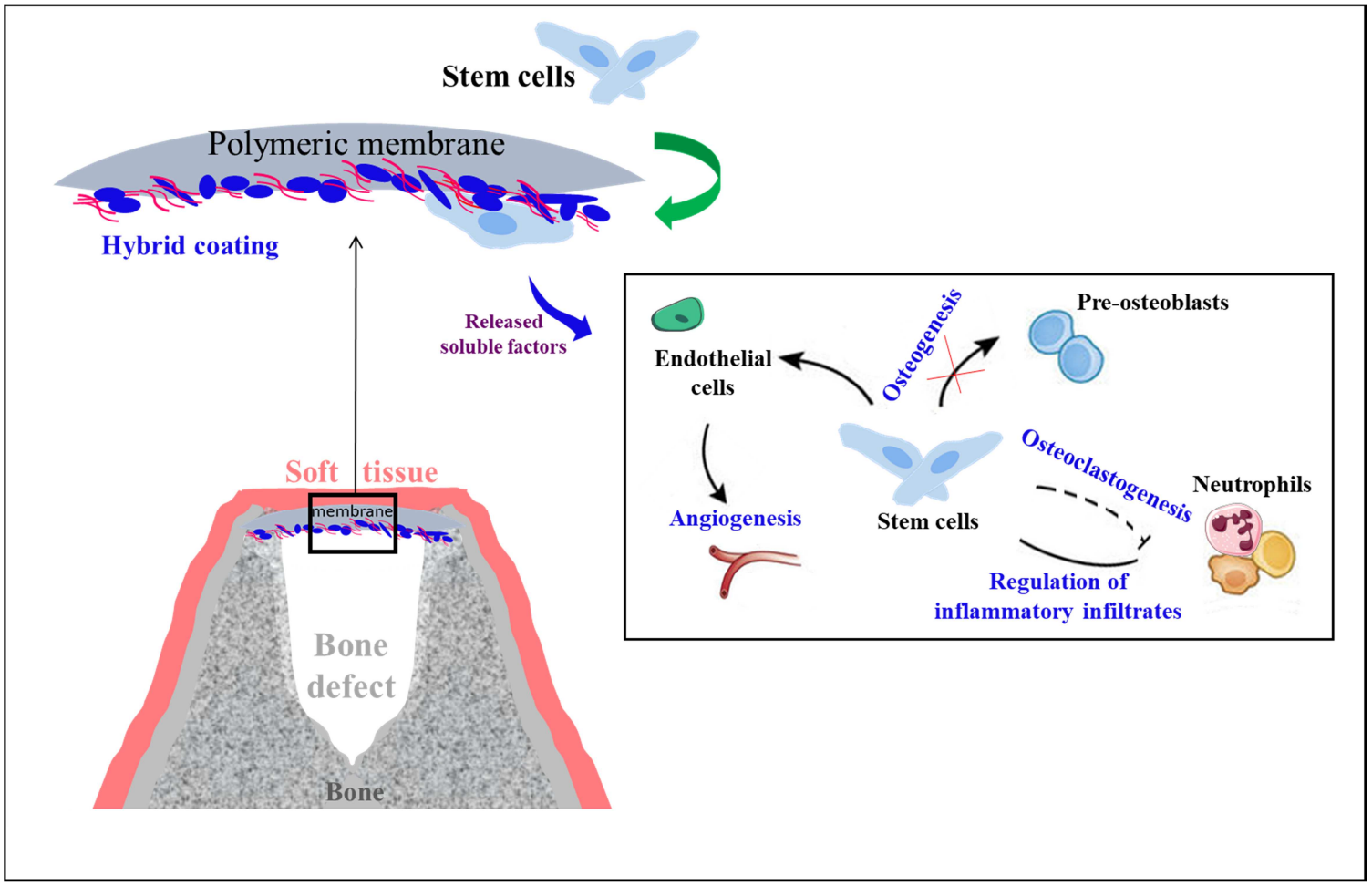
Stem cells
Polymeric membrane
Hybrid coating
Released
soluble factors
Soft tissue
membrane
Bone
defect
Bone
Endothelial
cells
Osteogenesis
Pre-osteoblasts
Angiogenesis
Stem cells
Osteoclastogenesis
Neutrophils
Regulation of
inflammatory infiltrates